GAP43, MARCKS, and CAP23 Modulate PI(4,5)P_2 at Plasmalemmal Rafts, and Regulate Cell Cortex Actin Dynamics through a Common Mechanism

Thorsten Laux,* Kiyoko Fukami,‡ Marcus Thelen,§ Tamara Golub,* Dunja Frey,* and Pico Caroni*

*Friedrich Miescher Institute, CH-4058 Basel, Switzerland; ‡Department of Biochemistry, Institute of Medical Sciences, Tokyo, Japan; and §Theodor Kocher Institut, Bern, Switzerland

Abstract. The dynamic properties of the cell cortex and its actin cytoskeleton determine important aspects of cell behavior and are a major target of cell regulation. GAP43, myristoylated alanine-rich C kinase substrate (MARCKS), and CAP23 (GMC) are locally abundant, plasmalemma-associated PKC substrates that affect actin cytoskeleton. Their expression correlates with morphogenic processes and cell motility, but their role in cortex regulation has been difficult to define mechanistically. We now show that the three proteins accumulate at rafts, where they codistribute with PI(4,5)P_2, and promote its retention and clustering. Binding and modulation of PI(4,5)P_2 depended on the basic effector domain (ED) of these proteins, and constructs lacking the ED functioned as dominant inhibitors of plasmalemmal PI(4,5)P_2 modulation. In the neuronlike cell line, PC12, NGF- and substrate-induced peripheral actin structures, and neurite outgrowth were greatly augmented by any of the three proteins, and suppressed by ΔED mutants. Agents that globally mask PI(4,5)P_2 mimicked the effects of GMC on peripheral actin recruitment and cell spreading, but interfered with polarization and process formation. Dominant negative GAP43(ΔED) also interfered with peripheral nerve regeneration, stimulus-induced nerve sprouting and control of anatomical plasticity at the neuromuscular junction of transgenic mice. These results suggest that GMC are functionally and mechanistically related PI(4,5)P_2 modulating proteins, upstream of actin and cell cortex dynamics regulation.

Key words: neurite outgrowth • cell spreading • anatomical plasticity • actin recruitment • lipid microdomain

Introduction

Signaling at the cell surface integrates specific contextual information from the local environment by recruiting and assembling cell-specific subplasmalemmal protein complexes that regulate cell behavior. To control signal quality and strength, cells assemble signaling platforms and structures of varying composition, complexity, and stability. Actin-based structures are major components of cell-surface signaling complexes such as focal contacts, adherens junctions, caps, and supramolecular activation clusters involved in lymphocyte activation, and synapses in the nervous system (Penninger and Crabtree, 1999). Since actin assembly is an early event in the formation of these signaling structures, defining mechanisms that regulate plasmalemmal actin dynamics, and the formation of transient and stable actin-based structures can provide significant insights into cell signaling.

Address correspondence to Pico Caroni, Friedrich Miescher Institute, Maulbeerstrasse 66, CH-4058 Basel, Switzerland. Tel.: 41-61-697-3727. Fax: 41-61-697-3976. E-mail: caroni@fmi.ch

At the cell surface, actin filament assembly and dynamics are subject to complex temporal and spatial control by signals from the extra- and intracellular environment (Welch et al., 1997; Schafer et al., 1998). Members of the Cdc42, Rac, and Rho family of small GTP-binding proteins couple cell-surface receptor activation to specific patterns of actin cytoskeleton regulation (Tapon and Hall, 1997). In addition, in cell-free systems, key actin binding and focal contact proteins such as gelsolin, profilin, cofilin, and vinculin are regulated by the lipid second messenger PI(4,5)P_2, which may be a critical component in promoting filament assembly at the cell membrane (Hartwig et al., 1995; Welch et al., 1997; Ma et al., 1998). However, since the overall contents of PI(4,5)P_2 at the inner leaflet of the cell membrane can be comparatively high and constant, it is not clear how this lipid second messenger regulates actin dynamics. Because of the relatively low affinities involved in these interactions, one critical parameter may be the local concentration of membrane PI(4,5)P_2 available for

ligand binding. Accordingly, one possibility for regulation would involve the existence of mechanisms to locally concentrate and mask $PI(4,5)P_2$ at the inner leaflet of the cell membrane, where its accessibility to actin regulatory proteins would be linked to extracellular signals.

GAP43, myristoylated alanine-rich C kinase substrate (MARCKS),[1] and CAP23 (GMC) are major protein kinase C (PKC) substrates associated with the plasma membrane that can bind acidic phospholipids including $PI(4,5)P_2$ (Skene, 1989; Aderem, 1995; Seki et al., 1996; Benowitz and Routtenberg, 1997; Denisow et al., 1998). Although they do not share regions of sequence homology, GAP43 can, to a large extent, substitute for CAP23 in vivo, indicating that the two proteins are closely related functionally (Frey et al., 2000a). Mechanistically, the function of GMC is still not understood, but loss- and gain-of-function studies in cell lines and mice argue for a critical role in regulating actin-based structures and motility (Aigner and Caroni, 1995; Aigner et al., 1995; Strittmatter et al., 1995; Stumpo et al., 1995; Myat et al., 1997; Frey et al., 2000a). Such a role is also consistent with the expression of these proteins, which is highly regulated during development and in the adult, and correlates with morphogenic processes and cell-surface dynamics (Skene, 1989; Aderem, 1995; Benowitz and Routtenberg, 1997; McNamara and Lenox, 1997). GMC share several characteristic properties such as the following: membrane association mediated by acylation; colocalization at unique subplasmalemmal patches; similar highly hydrophilic amino acid compositions; and the presence of a basic effector domain that binds acidic phospholipids, calmodulin, actin filaments, and PKC (Fig. 1 A; Hartwig et al., 1992; Aderem, 1995; Benowitz and Routtenberg, 1997; He et al., 1997; Wiederkehr et al., 1997). In artificial phospholipid vesicles, the effector domains (EDs) of MARCKS and GAP43 can bind and regulate the accessibility of acidic phospholipids, including $PI(4,5)P_2$, through electrostatic interactions (see e.g., Denisow et al., 1998). However, presently, experimental evidence that MARCKS and GAP43 regulate lipid second messengers at the cell membrane is lacking.

In this study, we present experimental evidence that GMC sequester and modulate $PI(4,5)P_2$ at cholesterol-dependent microdomains. Constructs lacking the ED acted as dominant inhibitors of microdomain $PI(4,5)P_2$ accumulation. The effects of GMC constructs on raft $PI(4,5)P_2$, peripheral actin recruitment, and neurite outgrowth were highly correlated, and were comparable to those of agents that directly affect $PI(4,5)P_2$. Based on these results, we propose that GMC are mechanistically related membrane-associated proteins that mediate calcium- and PKC-sensitive modulation of $PI(4,5)P_2$ at plasmalemmal microdomains, upstream of cell cortex and actin dynamics regulation, and neurite outgrowth. In the accompanying paper (Frey et al., 2000), we provide compelling evidence that GAP43 and the related protein CAP23 are related functionally in vivo, where they have common as well as unique functions in neurite outgrowth. Together, these studies establish GMC as members of a family of mechanistically and functionally related proteins. Because of their shared effects on $PI(4,5)P_2$ modulation, we propose the collective designation of pipmodulins.

[1]*Abbreviations used in this paper:* CaM, calmodulin; GMC, GAP23, MARCKS, and CAP23; MARCKS, myristoylated alanine-rich C kinase substrate; ED, effector domain; PKC, protein kinase C; PLC, phospholipase C.

Materials and Methods

Reagents, Cell Culture, and Transgenic Mice

Inhibitor compounds and growth factors, with their final concentrations, were used as follows. Neomycin (10 mM), NGF (100 ng/ml), cyclodextrin (methyl-β-cyclodextrin; 5 mM), and cytochalasin D (10 μM) from Sigma Chemical Co.; LiCl (10 mM) and calcimycin (50 μM) from FLUKA AG; and U-73122 (1 μM) from Calbiochem. For transfection, cDNAs were cloned into the eukaryotic expression vector pcDNA3 (Invitrogen). All mutant constructs were generated by conventional PCR techniques and verified by DNA sequencing. The MARCKS cDNA consisted of human MARCKS, with a modified C-term to match the chick sequence SPEGPAEPAE. Chick GAP43(ΔED) lacked amino acids 39–53; pMARCKS(ΔED) consisted of the human/chick protein, as described above, which lacked amino acids 152–176, and carried an additional Ala3Cys mutation to provide a palmitoylation sequence. Antisera to COOH-terminal peptides of chick MARCKS and GAP43 were as described (Wiederkehr et al., 1997). Mouse MARCKS was detected with an antiserum to the COOH-terminal synthetic peptide CSPEAPPAPTAE; the mAb to $PI(4,5)P_2$ was as described (Fukami et al., 1988); RITC-phalloidin, RITC-α-bungarotoxin, and Alexa-labeled secondary antibodies were from Molecular Probes, Inc.

Cell lines (monkey kidney epithelial cells COS-7, and rat pheochromocytoma PC12 cells, clone B) were from American Type Cell Culture Collection, and cultured in DME supplemented with 10% FCS, or 10% horse serum and 5% FCS, respectively. Hippocampal neurons were isolated from newborn (P0-1) mice. In brief, hippocampi were triturated, cells were washed, resuspended in culture medium (neurobasal; GIBCO BRL), with 0.5 mM L-glutamine, 25 μM glutamate, and 1% B27 supplement (GIBCO BRL), and plated at a density of 20,000 cells per 18-mm poly-L-lysine–coated coverslip.

Transgenic mice expressing chick GAP43(ΔED), specifically in adult neurons, were generated using the mouse Thy1.2 expression cassette as previously described (Caroni, 1997). Two independent lines of mice were analyzed in this study: line-13 expressed high levels of transgene (comparable to Thy1-GAP43(wt2); Aigner et al., 1995) in most types of neurons, including spinal motoneurons, whereas line-19 exhibited widespread expression in the brain and motoneuron at levels that were at least three times lower than those of line-13, as judged by immunoblots (brain) and immunocytochemistry (neuromuscular junction).

Transfections, Immunocytochemistry, and Analysis of the Actin Cytoskeleton

Liposome-based transfection reagents interfered with $PI(4,5)P_2$ stainings (not shown). Therefore, for transient transfections, COS-7 cells were treated with the nonliposomal reagent Superfect (Qiagen). On the next day, cells were fixed for 30 min at 37°C, followed by 3–5 h at 4°C with 4% paraformaldehyde in DME with 2 mM EGTA. Subsequently, cells were further processed for immunocytochemistry as described in a previous study (Wiederkehr et al., 1997). The first antibody binding incubation was carried out overnight at 4°C, using an antibody dilution solution consisting of PBS, with 0.2% saponin, 50 mM glycine, 0.1% BSA, and 1% FCS. Cultured hippocampal neurons from wild-type and transgenic mice were labeled 24 h after plating, according to the same protocol.

For quantitative analysis of GMC and $PI(4,5)P_2$ clusters, all cells from randomly selected fields (400×) with substantial levels of transgene expression (30–50% of all transgene expressing cells in any given field) were included in the analysis. At least 20 cells from one dish of transiently transfected cells were analyzed for every experiment, and the values are averages from at least two independent experiments. Images from 20 × 20 μm^2 bins were captured and all clusters within the bin were analyzed with NIH Image software (see Fig. 2).

PC12B cells were transfected stably using the Fugene 6 reagent from Boehringer. Each experiment shown in the study was carried out with at least three independent clones, with similar results. For process outgrowth assays, 100,000 PC12 cells were plated on collagen-coated (30 μg/ml) 35-mm dishes, and, where indicated, the medium was changed 1 d after plating from DME, 10% horse serum, 5% FCS (growth medium) to DME, 1%

horse serum, and 100 ng/ml NGF. Where process formation (>1 cell diameter) in the absence of NGF was monitored, cells were preincubated with or without neomycin for 2 h, replated in the presence or absence of the drug, and analyzed 3 h after replating. No preincubation was carried out when LiCl or the phospholipase C (PLC) inhibitor U-73122 was used.

To analyze the distribution of the actin cytoskeleton in PC12B clones, we determined intensity profiles of RITC-phalloidin labeling across randomly selected cells. Cells were plated on a collagen-coated substratum in the absence of NGF, fixed and stained 3 h after plating, photographed under identical conditions, and were analyzed with Image software. For each analyzed cell, one rectangular bin of 10 pixels in height was placed across the center of the cell (see also schematic in Fig. 6 B), and an edge-to-edge labeling intensity profile was collected. For each type of PC12B clone, such profiles had reproducible characteristic features of actin cytoskeleton distribution, as revealed when the profiles were superimposed. To highlight shared features, each of six independent profiles (i.e., six cells) was assigned the same light gray value, and overlapping areas were integrated (see Fig. 6 B).

Subcellular Fractionation and Lipid Analysis

Raft fractions from 2-d hippocampal neuron cultures or adult mouse brain homogenate were isolated according to a standard protocol (Maekawa et al., 1999). In brief, samples were processed with a Polytron homogenizer in hypotonic medium (10 mM Tris-HCl, 1 mM $MgCl_2$, 1 mM EGTA, with protease inhibitors), in the presence of 1% Triton X-100. The osmolarity was adjusted to 0.8 M sucrose (total volume of 3 ml), and the homogenate was overlayered with 0.7 M (5 ml), and no sucrose (2 ml) Triton-containing solutions. After centrifugation at 70,000 *g* for 6 h (4°C), the following three fractions were collected, sedimented in homogenization medium with 0.3% Triton X-100 (for 1 h at 100,000 *g*), and analyzed: (1) the fraction that had floated above 0.7 M sucrose (rafts); (2) 0.7 /0.8 M sucrose interface, plus upper 1 ml of 0.8 M sucrose layer (0.7/0.8 fraction); and (3) the gradient pellet (high density membranes and Triton-insoluble cytoskeleton; pellet fraction). Raft fractions from PC12B clones were isolated by an analogous protocol, but cell lysates were prepared in the presence of 150 mM NaCl, 1% Triton X-100 and 0.1 M sodium carbonate, pH 11.

Binding of GMC proteins to phospholipids was determined with a sedimentation assay, as described previously (Seki et al., 1996). In brief, multilamellar phospholipid vesicles were made from phosphatidylcholine (Sigma Chemical Co.) or from a 1:9 mixture of PC and PIP mix (PI(4,5)P2/PI(4)P/PI, 6:3:1; Sigma Chemical Co.), and incubated for 30 min at 30°C with 1 μg of bacterially expressed, purified His_6-tagged GMC protein in the presence of 150 mM NaCl (final volume, 150 μl, containing 4.5 μg PC, or 0.075 μg PC/PIP lipids). Vesicles with bound proteins were sedimented at 150,000 *g* for 30 min and analyzed on immunoblots.

Total masses of nonwater-soluble phosphoinositides were determined according to a standard protocol (Bird, 1998), using myo-(2-[^{3}H])-inositol (NEN) as a source of labeled inositol, PCA extraction, and TLC fractionation of phosphoinositides. The PI, PIP, and PIP2 spots were identified using phosphoinositide standards and iodine vapor. The appropriate spots were scraped off the TLC plates, extracted in ethanol/HCl (100:1), and counted in scintillation fluid. To compare PC12B clones, values were normalized to protein contents from parallel cultures. The PLC assay involved labeling with myoinositol, stimulation of cells with 20 μM bradykinin, and quantitative determination of the water-soluble breakdown products of labeled phosphoinositides by anion exchange chromatography as previously described (Bird, 1998). To compare PC12B clones, values were normalized to protein contents of acid-insoluble pellets. PIP_3 and $PI(3,4)P_2$ contents of NGF-treated PC12B clones were determined by [^{32}P]orthophosphate metabolic labeling and HPLC fractionation as described previously (Meier et al., 1998). PI(4)P levels were not affected by growth factor stimulation, and corresponding values were used to adjust individual sample counts per minute values for relative phosphoinositide recoveries.

Analysis of Peripheral Nerve Regeneration and BotA-induced Sprouting

To analyze peripheral nerve regeneration, the right sciatic nerve of 2–3-mo-old mice was crushed at the level of the midthigh, by applying pressure for 20 s with a watchmaker tweezer, as previously described (Aigner et al., 1995). Regeneration and reinnervation of muscle was analyzed 14 d after the crush, using a combined silver esterase reaction (Caroni et al., 1997) on frozen sections of triceps surae muscle. For quantitative analysis, the muscle was mounted slightly flattened, with the plane that faced the bone down; 50-μm sections of the entire muscle were cut, and at least 40 of these were analyzed, thus, covering all regions of the triceps surae muscle. Paralysis-induced nerve sprouting was analyzed as described (Frey et al., 2000). In brief, 0.01 U of botulinum toxin A (Allergan AG) was injected per gram of mouse into one triceps surae, and cryostat sections were analyzed with the combined silver esterase reaction 7 d after toxin treatment. Sprouting synapses in medial gastrocnemius and soleus were mapped systematically, and the results were displayed as percentages of synapses with sprouts along the synaptic band at a defined position of the muscle (Frey et al., 2000b).

Results

Codistribution of GMC with PI(4,5)P_2 at Plasmalemmal Microdomains

To determine whether subplasmalemmal clusters of GAP43, MARCKS, and CAP23 immunoreactivity may coincide with sites of local $PI(4,5)P_2$ accumulation, we carried out double labeling experiments with an antibody that binds specifically to $PI(4,5)P_2$ (Fukami et al., 1988). The antibody does not bind to PC, PE, PI, or IP_3, and only weakly to PI(5)P (Han et al., 1992). It binds to $PI(3,4,5)P_3$ with ~30% of the affinity that it has for $PI(4,5)P_2$, and does not bind to $PI(3,4)P_2$ nor PI(3)P (Fukami, K., unpublished results). In paraformaldehyde-fixed cells, the antibody yielded a patchy pattern of surface-associated immunoreactivity that was suppressed when cells were treated with agents that reduce (LiCl, calcimycin), or specifically mask (neomycin) plasmalemmal $PI(4,5)P_2$ (Fig. 1 B). When combined with the fact that $PI(3,4,5)P_3$ levels in cells are orders of magnitude lower than those of $PI(4,5)P_2$, these experiments validate the application of this antibody to specifically visualize plasmalemmal $PI(4,5)P_2$. As shown in Fig. 1 C, surface-associated $PI(4,5)P_2$ immunoreactivity codistributed precisely with clusters of endogenous or transgenic GMC immunoreactivity in hippocampal neuron growth cones and transfected COS cells. In addition, within any given cluster, there was a strong overlap of the four components.

Evenly patched GMC immunoreactivity patterns can be detected in both paraformaldehyde- or methanol-fixed cells (Wiederkehr et al., 1997). However, when cells were fixed with cold methanol, clusters were substantially smaller, suggesting that macroscopically detectable clusters may coalesce during the fixation and staining process. This is reminiscent of sphingolipid/GPI-linked protein microdomains (rafts), which have been shown to coalesce into larger aggregates during standard immunocytochemistry protocols (Harder and Simons, 1997; Harder et al., 1998). This is consistent with the possibility that GMC and $PI(4,5)P_2$ may colocalize at submicroscopic lipid microdomains; when double labeling experiments were carried out with glutaraldehyde-fixed cells, i.e., under conditions when macroscopically detectable clusters of GPI-linked proteins do not form (Harder et al., 1998), GMC and $PI(4,5)P_2$ exhibited nearly homogeneous surface labeling patterns (Fig. 1 C).

To determine whether GMC are raft components, we analyzed corresponding subcellular fractions from neonatal hippocampal neurons, mouse brain homogenates, and neuronlike PC12 cells. The GPI-linked cell-surface protein Thy1 is a well-characterized raft component (Harder and

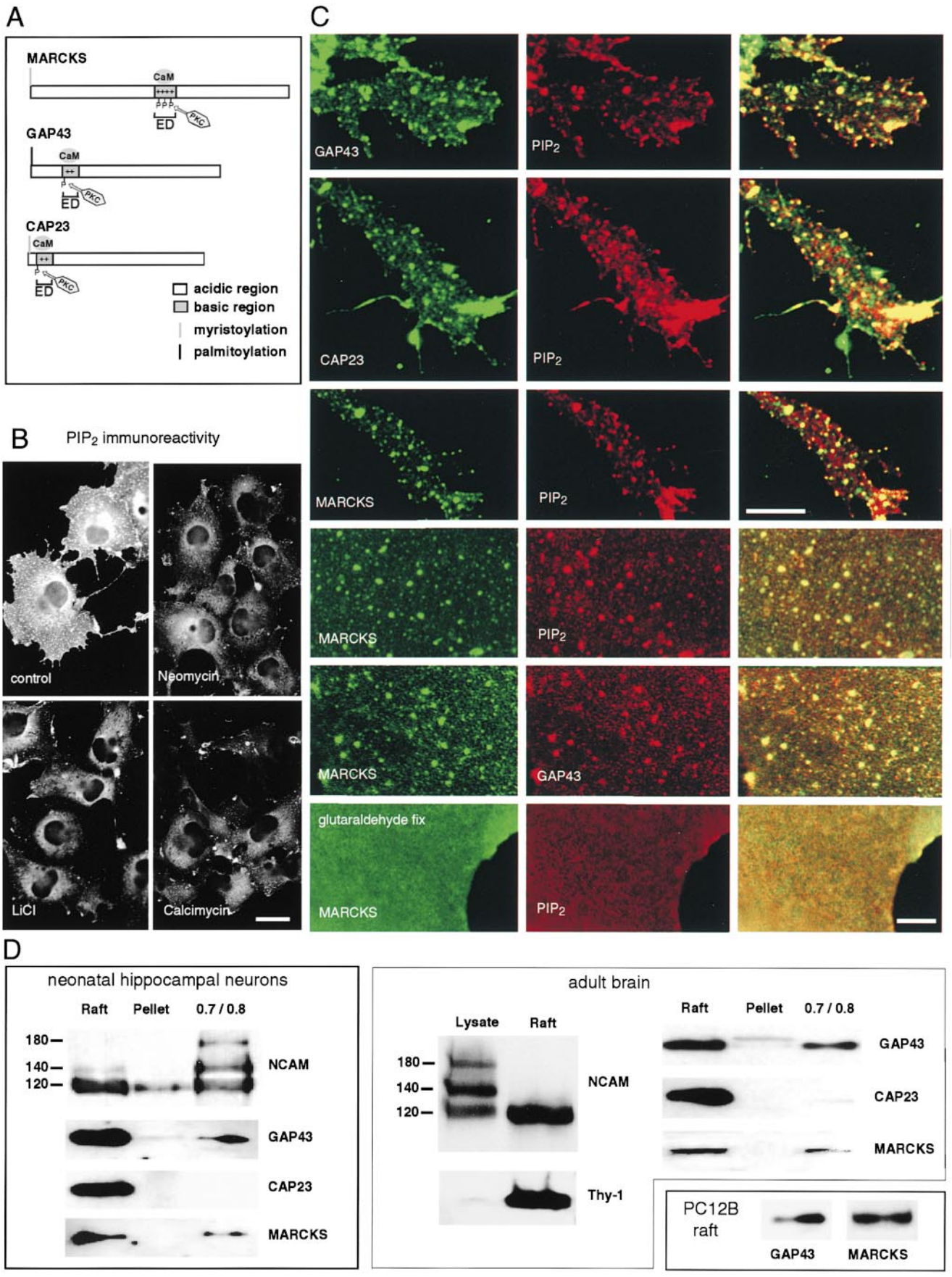
A
MARCKS
CaM
ED
PKC
GAP43
CaM
ED
PKC
CAP23
CaM
ED
PKC
acidic region
basic region
myristoylation
palmitoylation
B
PIP2 immunoreactivity
control
Neomycin
LiCl
Calcimycin
C
GAP43
PIP2
CAP23
PIP2
MARCKS
PIP2
MARCKS
PIP2
MARCKS
GAP43
glutaraldehyde fix
MARCKS
PIP2
D
neonatal hippocampal neurons
Raft
Pellet
0.7 / 0.8
180
140
120
NCAM
GAP43
CAP23
MARCKS
adult brain
Lysate
Raft
180
140
120
NCAM
Thy-1
Raft
Pellet
0.7 / 0.8
GAP43
CAP23
MARCKS
PC12B
raft
GAP43
MARCKS

Simons, 1997), and was highly enriched in the Triton-insoluble low density membrane raft fraction (Fig. 1 D). GPI-linked NCAM-120 is a raft component, whereas the NCAM-140 and NCAM-180 transmembrane isoforms are not (Olive et al., 1995). As shown in Fig. 1 D, the NCAM-120 isoform accumulated in the raft fraction, whereas the transmembrane isoforms did not, indicating that the raft fraction was selectively enriched for the appropriate subset of the membrane-associated proteins. GAP43, MARCKS, and CAP23 were all recovered in the raft fraction (Fig. 1 D). In addition, treating PC12 cells with cyclodextrin, an agent that sequesters cholesterol, thereby disrupting rafts, led to a loss of GAP43 in the raft fraction (see Fig. 2 C). Raft association was most pronounced for CAP23, whereas substantial fractions of total GAP43 and MARCKS were recovered in the 0.7/0.8 M sucrose fraction (Fig. 1 D). When brain tissue was homogenized in the absence of detergent, and separated into a soluble and a particulate fraction (100,000 *g*, 60-min pellet), about a third of MARCKS and GAP43, but not CAP23, were recovered in the soluble fraction (not shown). These findings are in good agreement with those from previous studies, and support the notion that most membrane-bound CAP23 and GAP43, and a substantial fraction of membrane-bound MARCKS are associated with plasmalemmal rafts. In addition, significant amounts of GAP43 and MARCKS are recovered in soluble fractions, and a fraction of membrane-bound MARCKS is associated with lysosomal compartments (Aderem, 1995). Taken together, these results support the notion that cell surface–associated microdomain GMC immunoreactivity reflects the association of these proteins with rafts at the inner leaflet of the cell membrane.

GMC Bind PI(4,5)P_2 and Promote PI(4,5)P_2 Microdomain Assembly Independent of Actin Cytoskeleton Integrity

To determine whether GMC can influence PI(4,5)P_2 -containing domains at the cell surface, we compared PI(4,5)P_2 labeling patterns in hippocampal neurons, PC12B cells, and COS cells expressing different levels of these proteins. As shown in Fig. 2 A, cells overexpressing GMC exhibited substantially larger macroscopic PI(4,5)P_2 clusters. In addition, MARCKS-overexpressing cells (but not those overexpressing GAP43 or CAP23; not shown) also exhibited stronger PI(4,5)P_2 cell-surface staining (Fig. 2 A). To exclude the possibility that the effects of GMC on the labeling pattern of PI(4,5)P_2 were related to the labeling process for these transgenes, we analyzed cells that had been transfected with a bicistronic construct driving the expression of the green fluorescent protein and MARCKS in the same transiently transfected cells. Cells expressing green fluorescent protein, and thus also MARCKS, exhibited larger, more numerous clusters and stronger labeling for PI(4,5)P_2 (not shown). Therefore, overexpression of GMC augments the formation of macroscopically detectable plasmalemmal PI(4,5)P_2 clusters.

To determine whether GMC proteins bind directly to PI(4,5)P_2, we carried out cosedimentation experiments with recombinant proteins and lipid vesicles. Binding of GMC to liposomes depended on the presence of acidic phospholipids such as PI(4,5)P_2, and on the presence of the basic ED (Fig. 2 B). Mutant GAP43(Ser42Asp), which does not bind calmodulin and codistributes with GMC at plasmalemmal microdomains (Wiederkehr et al., 1997), did bind to PI(4,5)P_2-containing vesicles, although less effectively than wild-type GAP43 (Fig. 2 B).

Cell-surface lipid microdomains described so far are highly sensitive to the physical properties of the lipid environment and, in particular, the presence of cholesterol (Harder and Simons, 1997). As shown in Fig. 2 C, treating COS cells with the cholesterol sequestering agent cyclodextrin, induced a loss of cluster and plasmalemmal PI(4,5)P_2. In transfected cells, this loss was accompanied by a concomitant reduction in the number and size of GMC clusters (Fig. 2 C). In addition, when compared with transgene-negative cells, overexpression of GAP43, MARCKS, or CAP23 partially protected cell surface and cluster PI(4,5)P_2 from cyclodextrin-induced dispersion (Fig. 2 C). In demonstrating that GMC-PI(4,5)P_2 cell-surface microdomains are highly interdependent, these results provide experimental evidence supporting the view that molecular interactions involving proteins such as GMC and phospholipids such as PI(4,5)P_2 are involved in the assembly and/or maintenance of these microdomains.

GAP43 and MARCKS can interact with actin filaments through their basic ED (Hartwig et al., 1995; He et al., 1997), and PI(4,5)P_2 interacts with a large number of actin-binding proteins (Welch et al., 1997). As a consequence, GMC may affect PI(4,5)P_2 microdomains through an indirect mechanism involving the actin cytoskeleton. To determine whether the association state of GMC-PI(4,5)P_2 microdomains depends on actin cytoskeleton integrity, we analyzed cluster size distributions in the presence of cytochalasin D. As shown in Fig. 3 A, treating COS cells acutely with 10 μM cytochalasin D for 20 min induced the loss of stress fibers and clumping of the actin cytoskeleton, but had no effects on PI(4,5)P_2 clusters, which remained significantly larger in the presence of MARCKS or GAP43. To investigate the effects of GMC on PI(4,5)P_2 microdomain assembly in the continued absence of an intact actin cytoskeleton, we analyzed COS cells cotransfected with GMC proteins and a constitutively active form

Figure 1. GAP43, MARCKS, and CAP23 accumulate at plasmalemmal rafts, where they codistribute with PI(4,5)P_2. (A) Schematic representation of GMC, with the relative position of the EDs. (B) Plasmalemmal immunoreactivity detected with the PI(4,5)P_2 antibody kt3g is suppressed by treatments that mask or reduce cell membrane PI(4,5)P_2. Treatment times are as follows: neomycin and LiCl, 24 h; and calcimycin, 15 min. (C) Codistribution of PI(4,5)P_2 immunoreactivity with endogenous GMC in hippocampal neuron growth cones and transiently transfected COS-7 cells. Note the absence of clustered labeling pattern for PI(4,5)P_2 and MARCKS in cells fixed with glutaraldehyde. (D) GMC accumulate in raft fractions from hippocampal neuron cultures, adult brain homogenate, and stably transfected PC12B clones. The samples are fractions from the sucrose density gradient used to isolate rafts; equal amounts of total protein were loaded on each lane. Lysate: brain homogenate. Bars: (B) 25 μm; (C) 3 μm.

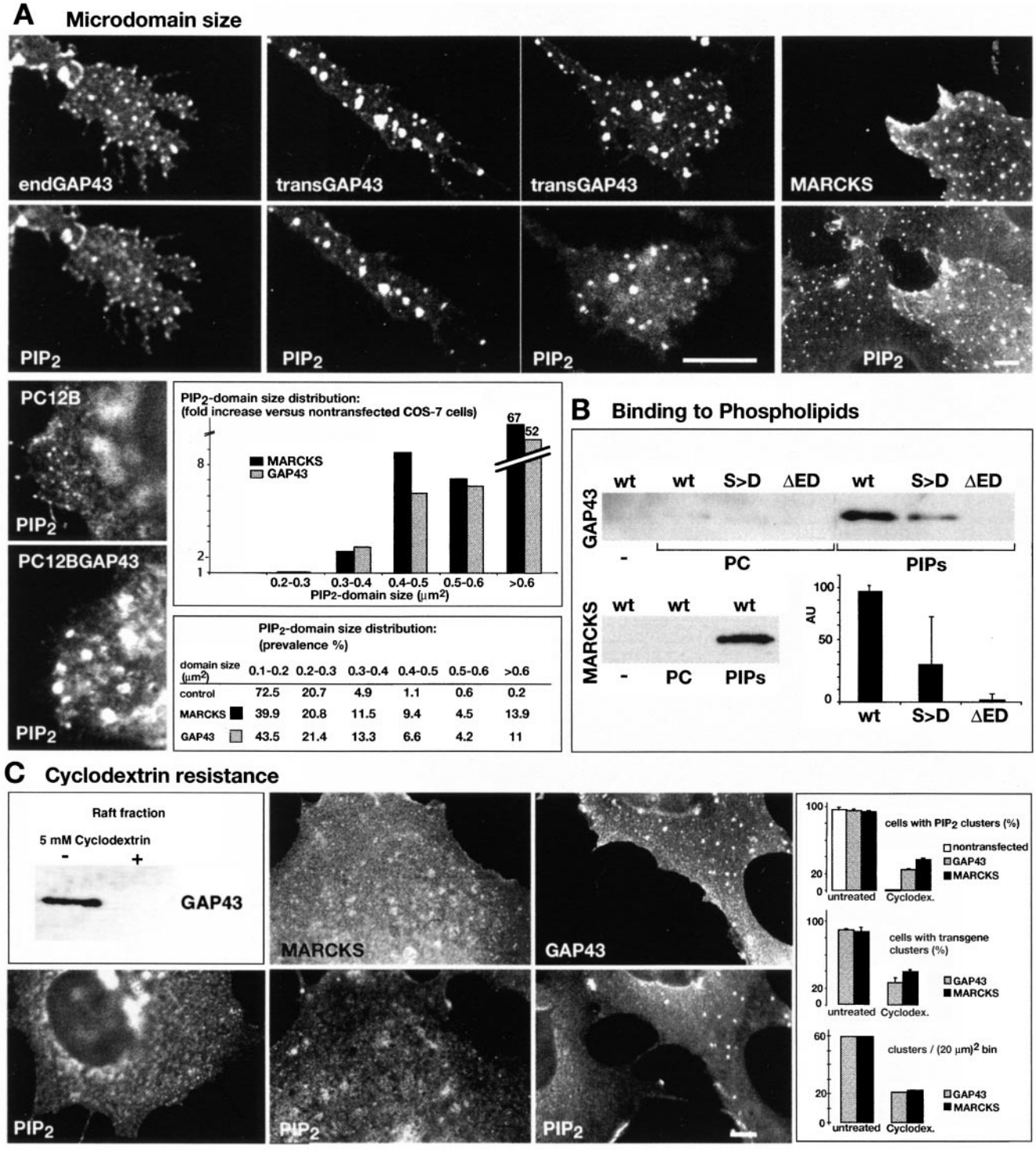

Figure 2. The distributions of PI(4,5)P_2 and GMC proteins at the cell membrane are interdependent. (A) Hippocampal neurons (left, nontransgenic; middle, transgenic overexpressing GAP43), COS cells (right) and PC12B cells overexpressing GMC proteins exhibit larger PI(4,5)P_2 clusters. Quantitative analysis: COS cells, one 20 × 20 μm^2 bin analyzed per cell (n = 20). (B) GAP43 and MARCKS bind to PI(4,5)P_2-containing (PIPs) but not to PC lipid vesicles; GAP43(Ser42Asp) binds more weakly; and GAP43(ΔED) does not bind. Quantitative analysis of GAP43 binding (immunoblot signal intensities, AU) to PIPs is shown in the graph (n = 4). (C) Cyclodextrin disperses plasmalemmal GMC-PI(4,5)P_2 microdomains; GMC protect partially against dispersion by cyclodextrin. Raft fractions: PC12B-GAP43 cells, immunoblot. Photographs: COS cells treated with cyclodextrin (5 mM, 30 min); left, nontransfected (compare to nontreated patterns in A). Quantitative analysis: COS cells, with and without cyclodextrin; one 20 × 20 μm^2 bin per cell (n = 40). Bars: 10 μm.

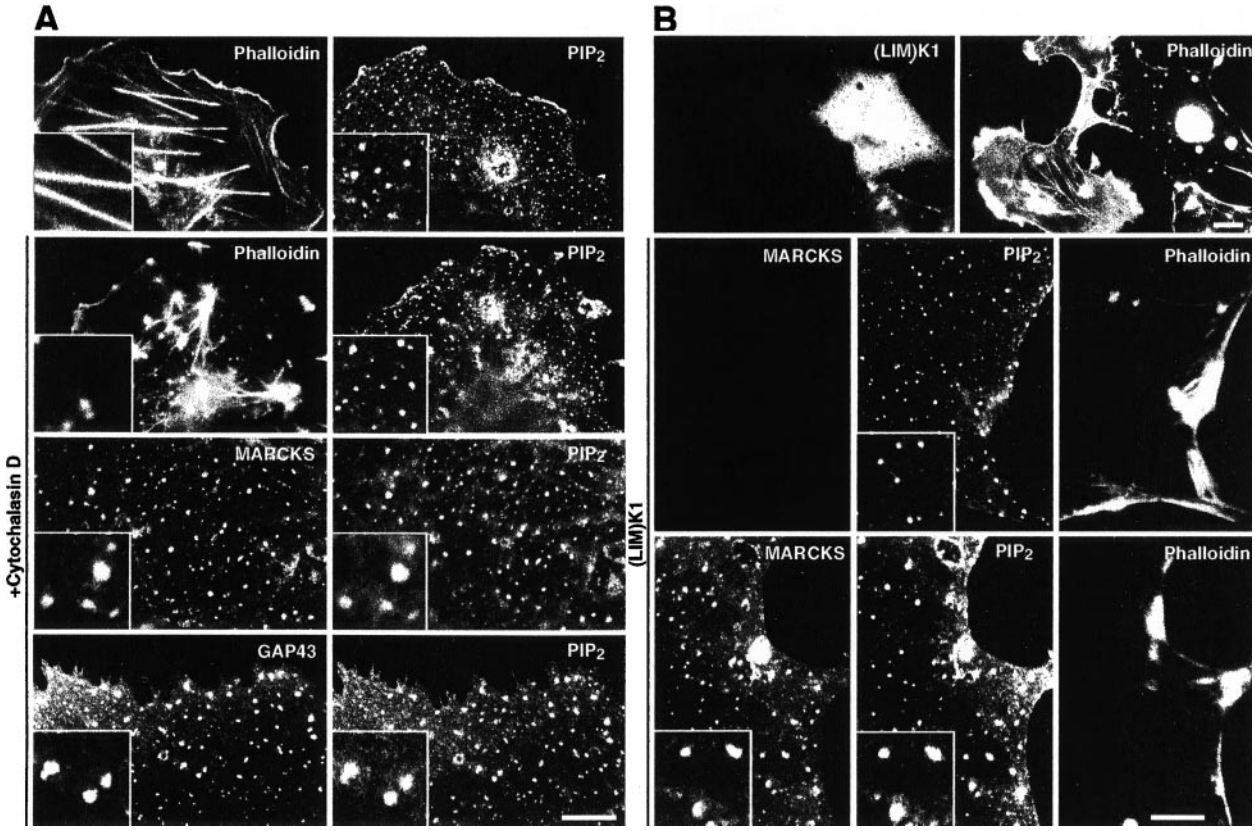

Figure 3. GMC modulate plasmalemmal PI(4,5)P_2 clusters independent of actin cytoskeleton integrity. Transiently transfected COS cells; (insets) details at 4×. Disruption of the actin cytoskeleton with cytochalasin D (20 min; A), or constitutively active (LIM)K1 (B) did not affect PI(4,5)P_2 clusters, nor the effect of GMC proteins (bottom panels in A, and bottom panels in B) on cluster size. (B, top panels) Actin cytoskeleton clumping in cells overexpressing (LIM)K1. (B, central and bottom panels) Triple labelings of cells overexpressing (LIM)K1 (clumped actin cytoskeleton), with or without MARCKS. Bars: 5 μm.

of LIM-kinase1 ((LIM)K1) that phosphorylates cofilin and blocks actin cytoskeleton dynamics (Arber et al., 1998). As shown in Fig. 3 B, cells overexpressing the (LIM)K1 construct, with or without MARCKS (or GAP43, or CAP23; not shown) exhibited massive collapsing of the actin cytoskeleton into a few large clumps, but GMC-PI(4,5)P_2 microdomains were not affected. Taken together, these results support the notion that GMC-PI(4,5)P_2 microdomain assembly and modulation is independent of the actin cytoskeleton.

MARCKS and GAP43 Mutants Lacking the Basic Effector Domain Reduce Microdomain Size and Interfere with PI(4,5)P_2 Retention at Plasmalemmal Clusters

GMC are acidic proteins, with one unique stretch of exclusively basic residues, that bind to acidic phospholipids like PI(4,5)P_2 (Fig. 2 A). Because of its palmitoylation, GAP43 does not require the presence of the ED to efficiently associate with the plasma membrane (Wiederkehr et al., 1997). In contrast, PKC-mediated phosphorylation or deletion of the ED leads to the dissociation of MARCKS and CAP23 from the plasma membrane (Thelen et al., 1991; Aderem, 1995; Laux, T., and P. Caroni, unpublished observations). Consequently, to generate a MARCKS (ΔED) construct that still associated with the plasmalemma, we introduced an Ala3Cys point mutation to generate palmitoylated pMARCKS(ΔED). In spite of the absence of the lipid-binding ED in the mutants, in double-transfected cells overexpressing MARCKS or GAP43, and GAP43(ΔED) or pMARCKS(ΔED), wild-type and mutant proteins codistributed at the cell surface (Fig. 4 A, bottom row). Therefore, accumulation of MARCKS or GAP43 at the characteristic surface-associated clusters, where these proteins colocalize, does not depend on the presence of the ED.

To explore the effects of the ED-free mutants on cluster assembly, we monitored their effects on PI(4,5)P_2 clusters. Cells expressing comparatively low levels of pMARCKS (ΔED) or GAP43(ΔED) exhibited cell-surface PI(4,5)P_2 immunoreactivity that colocalized with the mutant transgene at small clusters (not shown). In contrast, hippocampal neuron growth cones and COS cells expressing substantial levels of GAP43(ΔED) or pMARCKS(ΔED) exhibited transgene accumulation at numerous, regularly spaced, small plasmalemmal clusters, but were essentially devoid of plasmalemmal PI(4,5)P_2 clusters (Fig. 4, A and B). These results suggest that the presence of excess ED-free mutant interferes with the function of endogenous components involved in the recruitment of PI(4,5)P_2, and cluster coalescence. Since these mutants only differ from MARCKS or GAP43 by the absence of the ED that binds

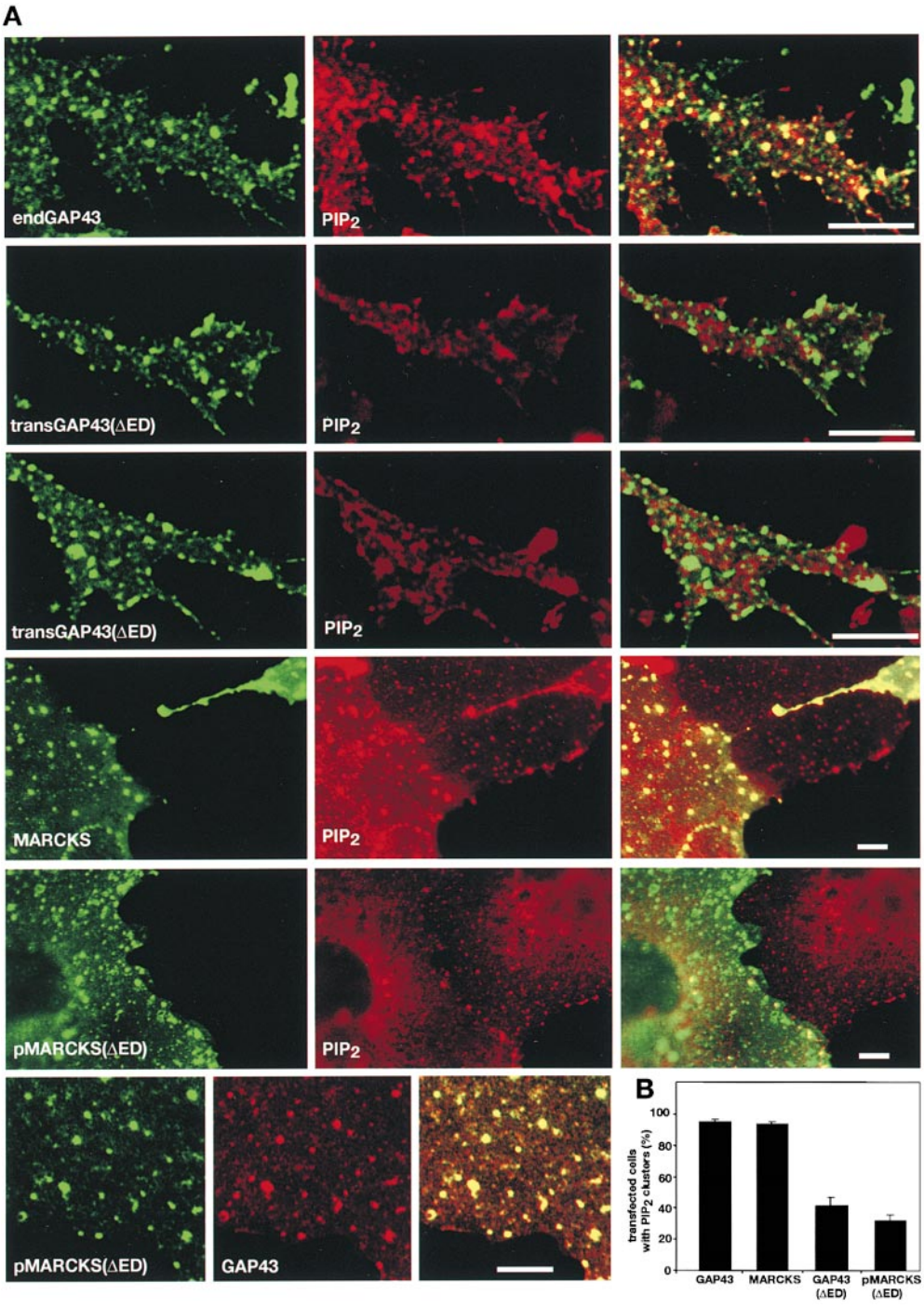

Figure 4. Mutants of MARCKS and GAP43 lacking the ED accumulate at GMC-PI(4,5)P_2 microdomains and interfere with PI(4,5)P_2 accumulation at the microdomains. (A, top three rows) Hippocampal neuron growth cones from wild-type (top) and Thy1-GAP43(ΔED) mice; bottom rows: single and double (bottom) transfections of COS cells, as indicated. (B) Quantitative analysis of transfection experiments; COS cells had up to 200–300 PI(4,5)P_2 clusters; cells with <10 clusters were scored as negative. n = 200. Bars: 5 μm.

to acidic phospholipids, it seems likely that interference is due to a dominant negative mechanism, involving accumulation of the competing, nonfunctional component at these PI(4,5)P_2 sequestering platforms.

PI(4,5)P_2 Microdomain Modulation by GMC Does Not Correlate with Alterations in Total Phosphoinositide Contents Nor Bradykinin-induced PI(4,5)P_2 Breakdown

We next determined whether overexpression of GMC constructs alters lipid second messenger metabolism. First, we determined the total sizes of the PI, PIP, and PIP_2 pools in stably transfected PC12B clones (Baetge and Hammang, 1991) overexpressing comparable amounts of MARCKS, GAP43, or dominant negative pMARCKS (ΔED) transgenes (see also Fig. 6). These cells express low levels of endogenous MARCKS and CAP23 (not shown) and extremely low levels of endogenous GAP43 (Baetge and Hammang, 1991). GAP43- or pMARCKS(ΔED)-overexpressing cells did not exhibit alterations in bulk phosphoinositide levels (Fig. 5 A). In contrast, overexpression of MARCKS produced a significant increase in phosphoinositide bulk levels in PC12B cells, a finding that is consis-

tent with the higher $PI(4,5)P_2$ immunoreactivity signals in cells transfected transiently with MARCKS. To determine whether overexpression of the GMC constructs affects signal-induced breakdown of $PI(4,5)P_2$, we analyzed bradykinin-induced $PI(4,5)P_2$ hydrolysis. This well characterized response to the activation of a G protein–coupled receptor involves the activation of PLC to hydrolyze $PI(4,5)P_2$ into inositol triphosphate and diacylglycerol. When compared with wild-type PC12B cells, the levels of stimulus-induced $PI(4,5)P_2$ metabolites were elevated in the presence of MARCKS, but not GAP43 (Fig. 5 B) nor pMARCKS (ΔED) (not shown). These results are consistent with the interpretation that MARCKS-overexpressing cells contain higher levels of the PLC substrate $PI(4,5)P_2$, whereas GAP43 or pMARCKS(ΔED) cells do not. Because GAP43 or pMARCKS(ΔED) overexpression did not alter bulk phosphoinositide levels nor stimulus-induced $PI(4,5)P_2$ breakdown, the results show that accumulation at $PI(4,5)P_2$-containing microdomains and augmentation or reduction of domain numbers and size does not, by itself, affect overall levels of $PI(4,5)P_2$ hydrolysis by activated PLC. As discussed below, the additional effects of MARCKS on bulk phosphoinositide levels may be due to the higher density of positive charges of its ED.

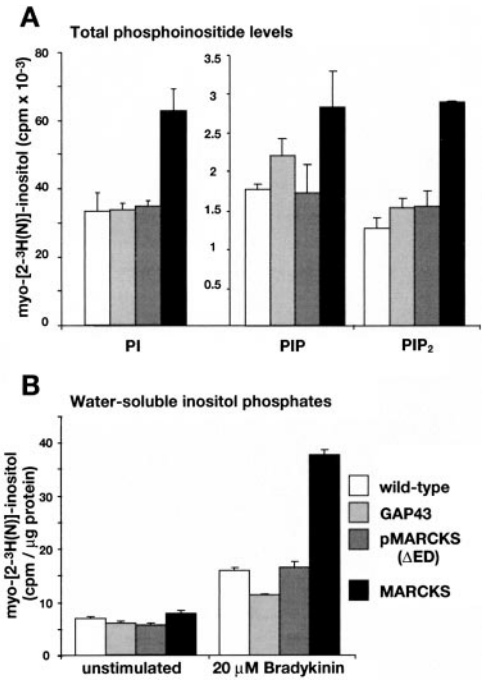

Figure 5. MARCKS, but not GAP43, nor pMARCKS(ΔED) affects bulk phosphoinositide contents in PC12B clones. (A) Bulk contents of PI, PIP, and PIP_2 (n = 4). (B) Bradykinin-induced (20 μM, 15 min) hydrolysis of $PI(4,5)P_2$ by PLC (n = 4).

Coordinate Regulation of $PI(4,5)P_2$ Microdomains and $PI(4,5)P_2$-sensitive Peripheral Actin Structures by GMC Constructs

GMC proteins and $PI(4,5)P_2$ have both been implicated in regulating the accumulation of actin structures at the plasmalemma (Hartwig et al., 1992; Aigner and Caroni, 1995; Hartwig et al., 1995; He et al., 1997; Welch et al., 1997; Wiederkehr et al., 1997). Modulation of microdomain $PI(4,5)P_2$ by GMC did not depend on the presence of an intact actin cytoskeleton (Fig. 3), which is consistent with the notion that it involves direct interactions between the EDs of GMC proteins and $PI(4,5)P_2$ at rafts. To explore the possibility that GMC modulation of plasmalemmal microdomain $PI(4,5)P_2$ may, in turn, regulate cell-surface actin dynamics, we analyzed the actin cytoskeleton of cells expressing GMC constructs. These experiments were carried out in neuronlike PC12 cells, where GAP43 promotes NGF-induced neurite outgrowth, a process that involves major rearrangements of the actin cytoskeleton (Paves et al., 1990). Three independent clones were analyzed for each construct, with comparable results. As shown in Fig. 6 and Fig. 7 A, overexpression of GAP43, GAP43(Ser42Asp), or MARCKS greatly potentiated the accumulation of actin-based filopodia and spikes at the periphery of untreated or NGF-treated PC12B cells. A comparison with wild-type PC12B clones revealed that, in the absence of NGF, this was accompanied by a dramatic decrease in cytosolic and perinuclear phalloidin signal (Fig. 6, A and B), suggesting the presence of a major shift towards the cell periphery in the subcellular accumulation of actin filaments. Indistinguishable results were obtained with PC12B clones overexpressing CAP23 (not shown). In marked contrast, GAP43(ΔED) or pMARCKS(ΔED) suppressed the accumulation of peripheral actin structures in response to NGF (Fig. 7 A). These findings are consistent with the view that $PI(4,5)P_2$ microdomain modulation by GMC promotes the assembly and accumulation of plasmalemmal actin-based structures.

To investigate more directly the possible involvement of $PI(4,5)P_2$ in GMC-regulated actin dynamics, we carried out experiments in the presence of 10 mM neomycin. This specific $PI(4,5)P_2$ sequestering agent (Fig. 1 B) had three major effects. First, it mimicked the overall effects of GMC on the distribution of the actin cytoskeleton, dramatically potentiating the accumulation of peripheral actin-based structures, particularly filopodia, at the plasmalemma, and greatly reducing the pool of comparatively amorphous cytosolic and perinuclear filamentous actin (Fig. 6, A and B, and Fig. 7 B). Second, it partially counteracted the effects of the dominant negative ΔED mutants (Fig. 7 B). Third, it counteracted the effects of GMC, with respect to the local accumulation of larger actin structures, cell polarization (Figs. 6 and 7 B), and neurite outgrowth (Fig. 8). As a result, cells treated with neomycin spread in radially symmetrical, round shapes, with dense accumulations of evenly distributed actin-based filopodia and lamellae at their edges. The effects of neomycin were mimicked most closely by the GAP43(Ser42Asp) mutant that does not bind calmodulin (CaM) and cannot be phosphorylated by PKC (Figs. 6 B and 7 A), suggesting that regulation of GMC proteins by calcium/CaM and PKC may promote the local accumulation of larger actin structures (see Fig. 10). The neomycin effects did not depend on the presence of NGF, which, like GMC proteins, potentiated the accumulation of larger peripheral actin structures, particularly spikes (Fig. 6 A). Interestingly, GMC and NGF had similar effects on neomycin-treated PC12 cells, and their combination partially rescued actin accu-

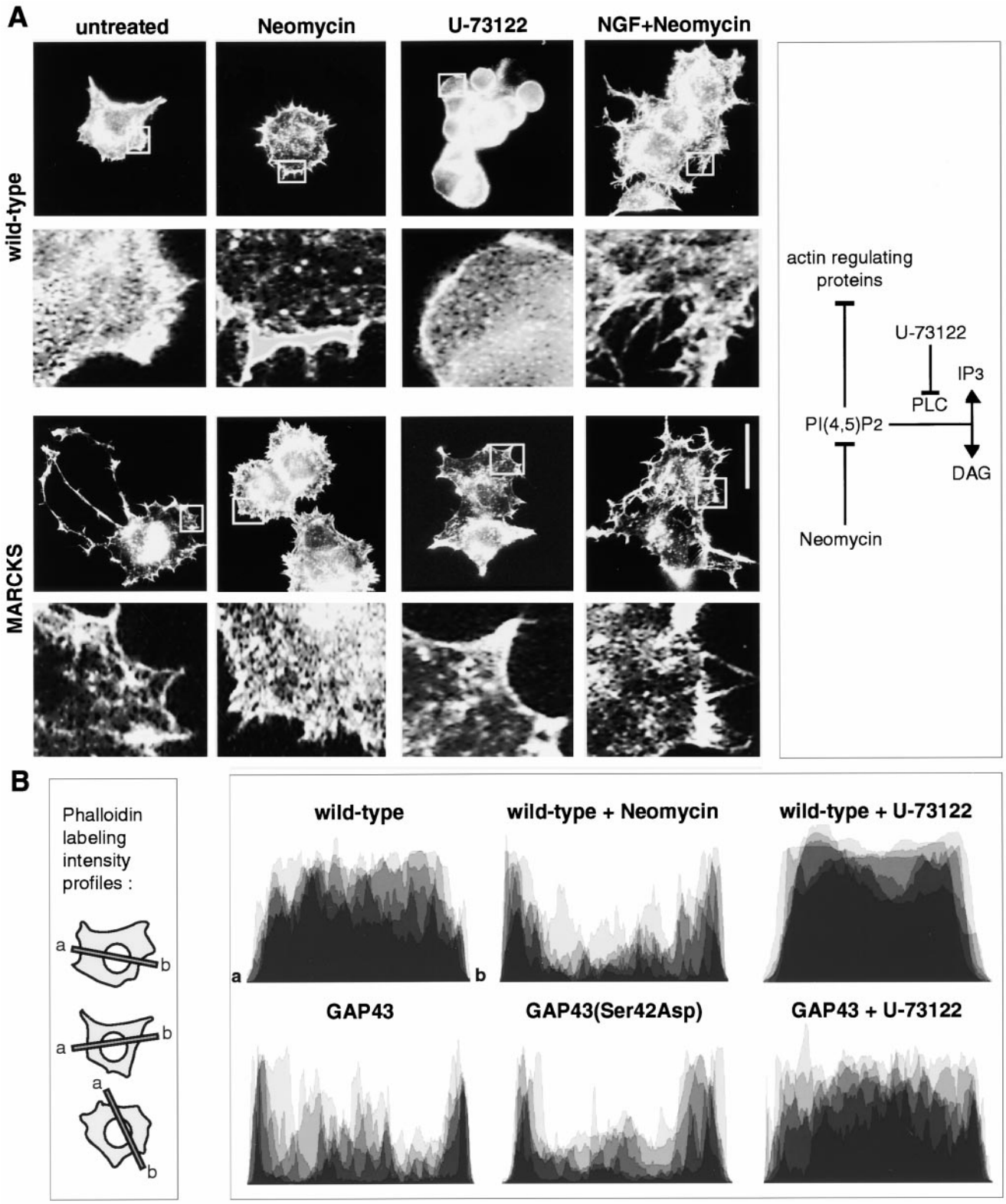

Figure 6. Roles of GMC and PI(4,5)P_2 in actin regulation at the cell periphery. (A) RITC-phalloidin patterns of PC12B cells 3 h after plating. The figure shows representative examples obtained with a clone expressing MARCKS; comparable results were obtained with GAP43 and CAP23 clones. (B) Quantitative analysis of phalloidin labeling profiles (see Materials and Methods for details). The schematic on the left shows how rectangular bins were placed (six cell profiles are superimposed for each plot on the right). Bar, 25 μm.

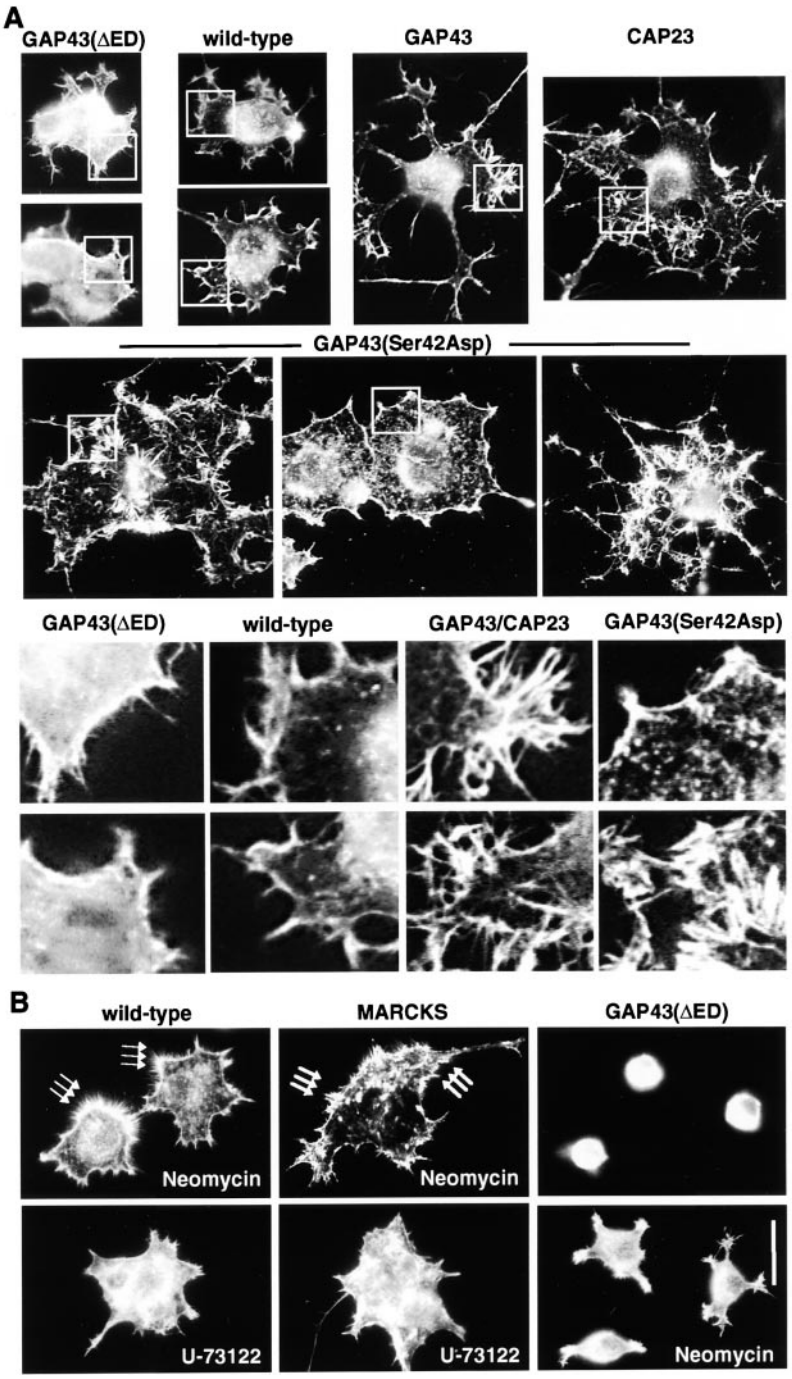

Figure 7. Opposite effects of GMC and their ΔED mutants on plasmalemmal actin dynamics. RITC-phalloidin labelings of PC12B clones. (A) Cells grown in the presence of NGF for 4 d. Rectangles show the position of the details shown in the bottom rows. (B) Cells grown for 1 d in the presence of NGF and drugs, as indicated. Note the induction of symmetrical actin structures in the presence of neomycin, partial rescue of polarization by MARCKS, and opposite effects of the PLC inhibitor U-73122. Also note that neomycin partially rescued peripheral actin accumulation in GAP43(ΔED) cells. Bar: 10 μm (A, top rows); 25 μm (B).

mulation polarity at the plasmalemma of these cells (Fig. 6 A), suggesting that with respect to actin regulation, GMC proteins and NGF may control synergistic pathways. Because it prevents the access of this enzyme to its substrate, neomycin is frequently used as an inhibitor of phospholipase C (PLC). However, direct inhibition of PLC with U-73122 had an effect opposite to that of neomycin: it reduced spreading and suppressed dynamic actin structures at the plasmalemma (Fig. 6, A and B, and Fig. 7 B). As discussed below (Fig. 6 A, schematic), these findings are consistent with the interpretation that, under local resting conditions, unmasked plasmalemmal $PI(4,5)P_2$ sequesters actin-regulating proteins that promote actin structure dynamics, thus, indirectly stabilizing the actin-based cortical cytoskeleton, and preventing the formation of dynamic actin structures involved in protrusive activity and spreading.

Critical Role of Plasmalemmal GMC for Neurite Outgrowth in PC12 Cells

To investigate possible biological implications of microdomain and actin regulation by GMC proteins, we analyzed NGF-induced neurite outgrowth in stable PC12B clones overexpressing wild-type and ED-deficient con-

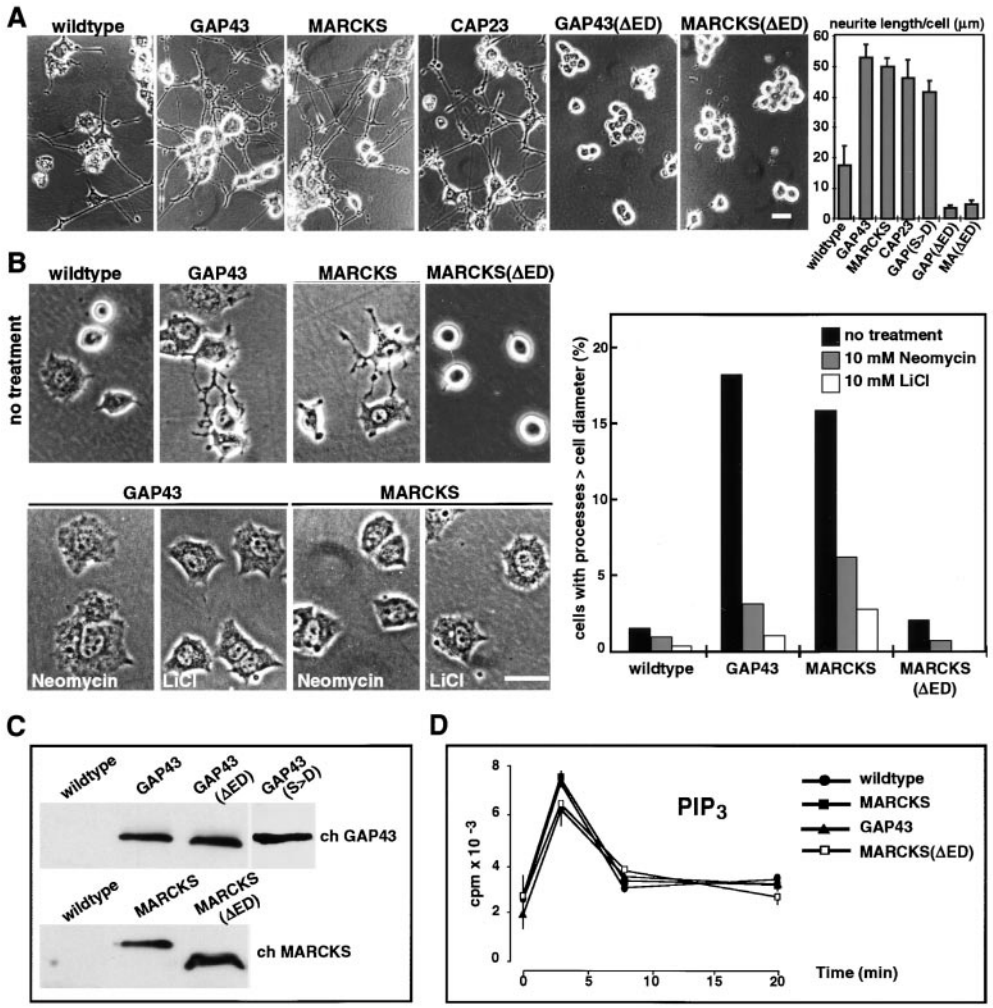

Figure 8. Role of GMC proteins in neurite outgrowth in PC12B cells. (A) NGF-induced neurite outgrowth (4-d cultures). Quantitative analysis: 150 neurons per 4-d culture (N = 4). (B) Spreading and process outgrowth in the absence of NGF; cells 3 h after plating on a collagen-coated substrate. Neomycin and LiCl promoted symmetrical cell spreading and suppressed process outgrowth. Quantitative analysis of the data: all cells (total ~500) from randomly selected fields. (C) Transgene expression levels (immunoblots) in the PC12B clones shown in Figs. 6–8. Equal amounts of total protein per lane. (D) Induction of PIP_3 synthesis in NGF-treated PC12B clones. Note indistinguishable induction of this PI3-kinase product in the clones (n = 6). Bars: 25 μm.

structs. As expected (Yankner et al., 1990), overexpression of GAP43 substantially potentiated cell spreading and neurite outgrowth (Fig. 8 A). MARCKS- or CAP23-overexpressing cells exhibited potentiated neurite outgrowth indistinguishable from that induced by GAP43 (Fig. 8 A). This is remarkable, given the absence of sequence homologies between the three proteins, and is consistent with their similar effects on $PI(4,5)P_2$-containing microdomains and the actin cytoskeleton. Dominant negative GAP43(ΔED) or pMARCKS(ΔED) suppressed NGF- induced neurite outgrowth (Fig. 8 A). These findings are entirely consistent with the effects of GMC constructs on $PI(4,5)P_2$-containing microdomains and actin dynamics, and provide evidence for a critical role of GMC protein-mediated regulation in neurite outgrowth.

To determine whether GMC can induce process outgrowth in these cells in the absence of NGF, we monitored attachment and spreading of PC12 clones on a collagen substratum. Unlike wild-type cells, GMC-overexpressing cells formed neuritelike processes during spreading in the presence of high serum concentrations and no NGF (Fig. 8 B). Under these experimental conditions, process formation was transient: it peaked at ~3 h after plating, and processes disappeared after 15 h (not shown). In contrast to those formed in the presence of NGF, processes were short, not exceeding 50 μm in length, and were not affected by the presence of the PI3-kinase inhibitor LY294002 (not shown). The specific $PI(4,5)P_2$ sequestering agent neomycin promoted symmetrical cell spreading, and prevented spontaneous process formation (Fig. 8 B) and NGF-induced neurite outgrowth (not shown, but see Fig. 7 B) in GMC-overexpressing cells. Comparable effects were obtained with 10 mM LiCl (Fig. 8 B), which inhibits the metabolism of phosphoinositides, and greatly reduces the levels of plasmalemmal $PI(4,5)P_2$ (Fig. 1 B). In contrast to neomycin, U-73122, which directly inhibits PLC, effectively inhibited cell spreading (see also Fig. 6 A).

NGF-induced neurite outgrowth involves the activity of PI3-kinases (Jackson et al., 1996), which may depend, in part, on the local concentrations of plasmalemmal substrate phosphoinositides available for phosphorylation. However, neither GMC proteins nor their ΔED mutants affected the accumulation of the 3-phosphoinositides PIP_3 (Fig. 8 D) or $PI(3,4)P_2$ (not shown) in response to NGF, which is consistent with the notion that the regulation of neurite outgrowth by GMC proteins specifically involves $PI(4,5)P_2$.

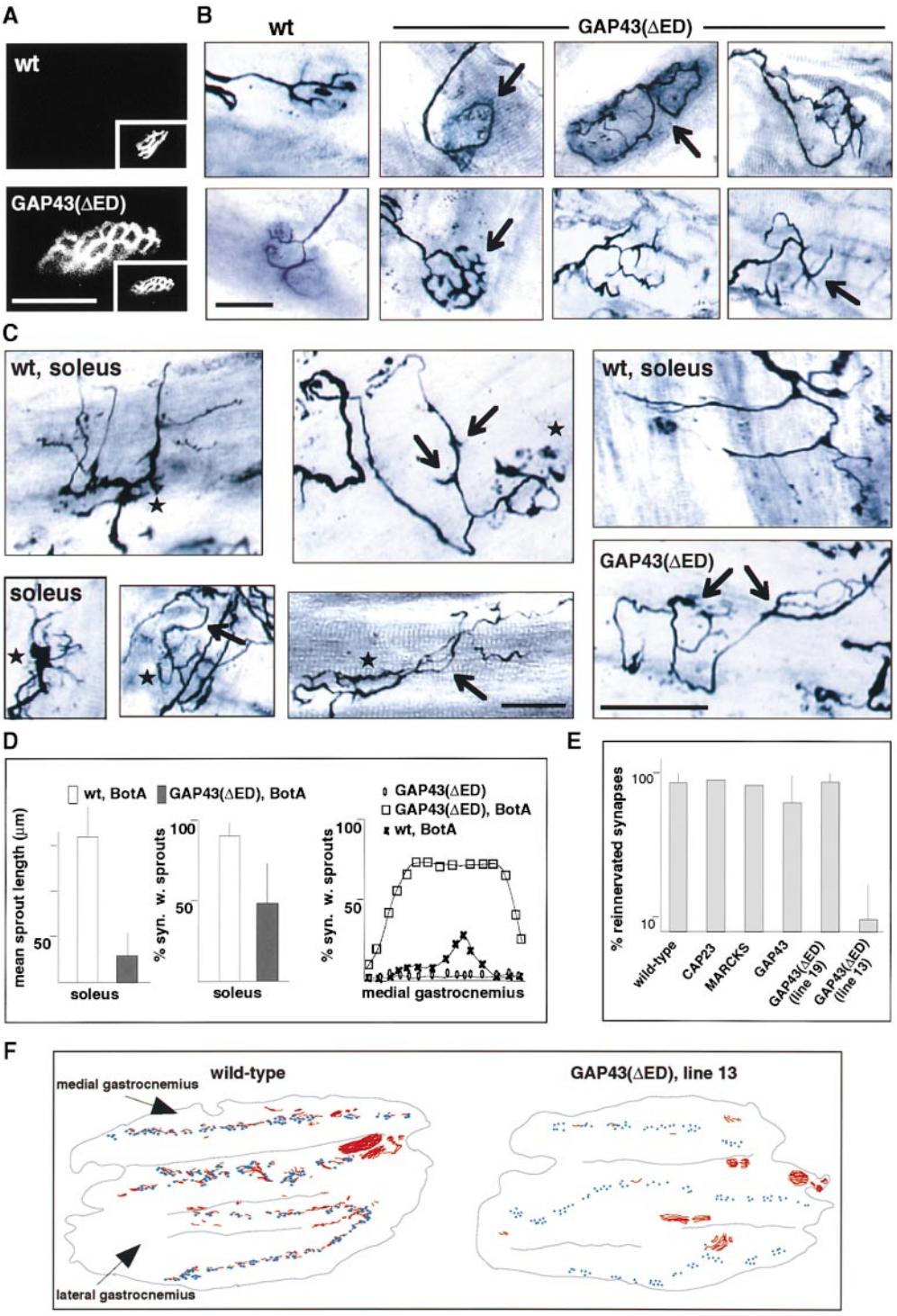

Figure 9. Role of GMC-mediated regulation in anatomical plasticity and peripheral nerve regeneration. (A) Expression of GAP43(ΔED) at the adult neuromuscular junction (medial gastrocnemius muscle). (insets) Same synapse visualized with RITC–α-bungarotoxin. (B) Neuromuscular junction configurations at medial gastrocnemius of wild-type and Thy1-GAP43(ΔED) mice (line-13). Note circular shapes and enlargements of nerve terminal branches in the mutants (arrows). (C) Synaptic sprouting 7 d after BotA treatment. The photographs show sprouts in medial gastrocnemius (or soleus, where indicated) of Thy1-GAP43(ΔED) mice (or wild-type mice (wt), where indicated)). The two panels on the right show details of sprouts. (arrows) Unusual features of sprouts in the presence of GAP43(ΔED) (curved, lamellae, and side branches); and (asterisk) neuromuscular junctions. (E) Reinnervation of triceps surae, 14 d after nerve crush in wild-type and Thy1 transgenic mice, as indicated. Neuromuscular junction transgene immunoreactivity in line-13 was about threefold higher than in line-19, and comparable to that of the other transgenic lines included in the analysis ($n = 4$). (F) Representative camera lucida of triceps surae reinnervation 14 d after sciatic nerve crush. The synaptic band (acetylcholine esterase reaction product) is in blue, and nerve profiles (silver stain) are in red. Bars: 25 μm.

Role of GMC-mediated Regulation in Peripheral Nerve Regeneration and Stimulus-induced Nerve Sprouting at the Neuromuscular Junction in the Adult

Although GAP43 has been implicated in axonal growth, GAP43-deficient mice only exhibit restricted axonal pathfinding defects (Strittmatter et al., 1995; Sretavan and Kruger, 1998). Likewise, MARCKS-deficient mice do form axonal projections, although these are highly aberrant (Stumpo et al., 1995). Our results (Frey et al., 2000a) provide strong evidence that these proteins have partially redundant functions, suggesting that to reveal their full functional roles would require approaches that interfere with common downstream components. Therefore, we generated transgenic mice overexpressing dominant negative GAP43 (ΔED) specifically in neurons. We used a mouse Thy1.2 expression cassette, thus, achieving high expression levels restricted to postnatal neurons, including motoneurons and their neuromuscular synapses (Fig. 9 A; Caroni, 1997). Hippocampal neurons derived from such mice exhibited a disruption of growth cone plasmalemmal $PI(4,5)P_2$ clusters

(Fig. 4 A), and extended neurites of greatly reduced length (<30% of wild-type values; not shown).

In control wild-type mice, nerve terminal branches at the neuromuscular junction exhibit a regular decrease in diameter as they elongate towards the periphery of the synapse (Fig. 9 B). This characteristic pattern was detected at most adult gastrocnemius muscle synapses that we examined (at least 465/500 synapses from three mice). In contrast, in GAP43(ΔED)-overexpressing mice, nerve terminal branches were irregular in shape, with frequent enlargements at their tips (Fig. 9 B). In addition, the nerve frequently exhibited a strikingly circular course (Fig. 9 B). The circular course was reminiscent of CAP23−/− neurons, where the phenotype could be phenocopied by cytochalasin D, supporting the notion that it was due to a defect in the actin cytoskeleton (Frey et al., 2000a).

GAP43 and CAP23 promote nerve sprouting at the neuromuscular junction (Aigner et al., 1995; Caroni et al., 1997; Frey et al., 2000a). To determine the effect of GAP43(ΔED) on stimulus-induced nerve sprouting, we paralyzed lower hindlimb muscles of transgenic mice with botulinum toxin A. 7 d after toxin treatment, >95% of the synapses in the soleus muscle of wild-type mice exhibit robust ultraterminal sprouting, whereas sprouting in the medial gastrocnemius is much less pronounced, and is restricted to slow-type synapses (Frey et al., 2000b; Fig. 9, C and D). As predicted, sprouting in the soleus muscle of transgenic mice was greatly reduced in frequency and length (Fig. 9, C and D). However, in addition, a large proportion of medial gastrocnemius synapses that do not sprout in wild-type mice, nor in Thy1-GAP43 mice (Frey et al., 2000b), did so in the presence of GAP43(ΔED) (Fig. 9 D). Sprouting in the absence of toxin treatment was minimal (Fig. 9 D), suggesting that the presence of GAP43(ΔED) interfered with negative control of stimulus-induced sprouting at these synapses. When compared with those induced in wild-type mice, sprouts were strikingly curved, with frequent side branches and local expansions (Fig. 9 C). Again, these features were reminiscent of the abnormal neurite outgrowth patterns in CAP23−/− or cytochalasin D–treated neurons (Frey et al., 2000a), which is consistent with the notion that they may reflect a disruption in actin cytoskeleton control at the cell cortex.

Finally, to explore the role of GMC proteins in axonal regeneration, we crushed the sciatic nerve of Thy1-GAP43 (ΔED) mice and monitored peripheral nerve regeneration. As shown in Fig. 9 (E, F), GAP43(ΔED) inhibited regeneration and reinnervation of skeletal muscle in a dose-dependent manner. Ultrastructural analysis of myelinated axonal profiles proximal to the crush site revealed normal numbers in the mutant mice (not shown). In addition, although with a substantial delay, skeletal muscle was apparently fully reinnervated also in the transgenic line expressing high levels of GAP43(ΔED). Therefore, the presence of excess GAP43(ΔED) greatly delayed, but did not completely prevent peripheral nerve regeneration. These results are consistent with the in vitro data with PC12 cells, and indicate that regulation by GMC proteins plays a critical role in axonal outgrowth in vivo.

Discussion

We have provided evidence that GAP43, MARCKS, and CAP23 regulate plasmalemmal microdomain $PI(4,5)P_2$, cell cortex actin recruitment, and morphogenic processes such as neurite outgrowth. The effects of GMC constructs on the actin cytoskeleton and morphogenic processes correlated closely with those on plasmalemmal $PI(4,5)P_2$, and were mimicked by pharmacological agents that act on $PI(4,5)P_2$, which is consistent with the notion that a main function of these proteins is to locally modulate $PI(4,5)P_2$, upstream of actin cytoskeleton and cell cortex regulation. In the following sections, we discuss the regulation of $PI(4,5)P_2$ microdomains by GMC-like proteins and their function in actin dynamics, neurite outgrowth, and anatomical plasticity.

A Lipid Microdomain that Brings Together PI(4,5)P_2 and the Plasmalemma-associated Proteins GAP43, MARCKS, and CAP23

The results of this study suggest that $PI(4,5)P_2$ and GMC proteins accumulate together at a subtype of cholesterol-rich plasmalemmal microdomains found in many, and possibly all types of cells. Thus, endogenous and transgenic GMC accumulated in cyclodextrin-sensitive raft fractions (Fig. 1 D; Maekawa et al., 1999), where they codistributed with $PI(4,5)P_2$ (Liu et al., 1998; Pike and Miller, 1998) in a surface-associated patchy pattern in all cell lines and primary cell types that we have tested. This characteristic pattern did not overlap with the distribution of a number of surface-associated components, including early endosomes, caveolin, integrin-β1, and vinculin, which also yield patchy labeling patterns. The microdomains described in this study appear to share significant physico-chemical properties with sphingolipid/GPI-linked protein microdomains (Harder and Simons, 1997). However, the absence of substantial colocalization between GMC-$PI(4,5)P_2$ and src or caveolin (Wiederkehr et al., 1997) suggest that these microdomains may not overlap physically with sphingolipid/GPI-linked protein rafts, and that GMC-$PI(4,5)P_2$-containing microdomains may belong to a subtype of rafts.

Definitive information about the properties and the regulation of GMC-$PI(4,5)P_2$ microdomains will require further studies, including their biochemical isolation, and molecular identification of their lipid and protein components, as well as a characterization of their dynamic properties. However, some conclusions can already be drawn from this study. First, like previously described rafts, they are sensitive to cholesterol-depleting drugs, implying that significant domain promoting forces possibly related to those operating in sphingolipid rafts reside within the lipid environment. Second, direct interactions between $PI(4,5)P_2$ and GMC proteins appear to promote $PI(4,5)P_2$ retention at the domains. Thus, overexpression of GMC, induced larger macrodomains, and partially counteracted cyclodextrin-induced loss and dispersion of plasmalemmal $PI(4,5)P_2$. In contrast, effector domain mutant accumulation may reduce the net binding capacity of the domain for $PI(4,5)P_2$, thus, reducing masking and retention of this lipid second messenger. Along similar lines, the higher total contents of $PI(4,5)P_2$ in MARCKS, but not in GAP43-overexpressing cells may be due to the fact that the ED of MARCKS has a significantly higher density of basic residues (13 lysine and arginine out of a total of 25 residues in

MARCKS, versus 8/23 in GAP43), thus, binding $PI(4,5)P_2$ with higher avidity. These combined findings suggest that direct electrostatic interactions between the ED-containing proteins and acidic phospholipids, including $PI(4,5)P_2$, may be involved in domain stabilization. However, additional, presently unidentified, components are likely to be involved in microdomain nucleation and recruitment. Thus, for example, since mutant constructs of MARCKS or GAP43 lacking the ED codistribute with the wild-type proteins and $PI(4,5)P_2$, protein interactions not involving the ED must be involved in GMC targeting to these domains.

With respect to their regulation, an important difference to previously described rafts is that while sphingolipid/GPI-linked protein complexes occupy the outer leaflet of the plasmalemma, where they can be regulated by signals from the extracellular environment, GMC-$PI(4,5)P_2$ complexes are located at the inner leaflet. The interaction of the basic domains of GMC with acidic phospholipids, including $PI(4,5)P_2$, is subject to regulation by several signaling pathways (Aderem, 1995; Benowitz and Routtenberg, 1997). Accordingly, phosphorylation by PKC or binding of calcium/CaM would mimic ED deletion by masking positively charged EDs, thereby weakening electrostatic interactions that sequester $PI(4,5)P_2$. As a consequence, GMC proteins may mask and inhibit microdomain $PI(4,5)P_2$ under resting conditions, and release clustered $PI(4,5)P_2$ in response to local calcium/CaM and/or PKC activation (Fig. 10).

Functions of GMC Proteins in Actin Regulation, Neurite Outgrowth, and Anatomical Plasticity

The question of whether GMC are signaling or structural proteins, and what, if any, are their downstream targets has been difficult to address experimentally in the past. Because they can be such abundant proteins, and because their EDs interact with several molecules involved in signaling, including calcium/CaM, PKC, $PI(4,5)P_2$, and actin filaments, it has been suggested that MARCKS and GAP43 may regulate the pools of any of these interacting molecules. However, we now find that GMC can modulate $PI(4,5)P_2$ independent of binding to CaM or actin cytoskeleton integrity, and that all effects of GMC on the actin cytoskeleton, cell spreading and neurite outgrowth correlate with their effects on microdomain $PI(4,5)P_2$. The global effects on cell spreading and peripheral actin recruitment are mimicked by drugs that reduce the availability of $PI(4,5)P_2$, whereas the effects on cell polarization and process formation are, in part, prevented by these same drugs. This may reflect the regulatory cycle outlined above, i.e., masking of $PI(4,5)P_2$ under resting conditions, which is mimicked by neomycin, and local unmasking of clustered $PI(4,5)P_2$ in response to calcium/CaM and/or PKC activation, which is not mimicked by neomycin (Fig. 10). This interpretation is also consistent with the observation that GAP43(Ser42Asp), which does not bind CaM, cannot be regulated by PKC, but still binds $PI(4,5)P_2$, affected the actin cytoskeleton in a manner that was particularly reminiscent of that of neomycin (Figs. 6 B and 7 A). Therefore, we propose that $PI(4,5)P_2$ is a main effector of GMC, and that, rather than being regulated by GMC, calcium/CaM and PKC regulate the interactions of GMC with $PI(4,5)P_2$. Accordingly, a main function of GMC would be to act as $PI(4,5)P_2$ modulatory pipmodulins, to retain and mask $PI(4,5)P_2$ at plasmalemmal lipid microdomain platforms, where they would couple its availability for actin cytoskeleton and cell cortex regulation to signal transduction pathways involving calcium/CaM and PKC (Fig. 10). In addition to modulating $PI(4,5)P_2$, MARCKS and GAP43 can also interact directly with actin filaments (Hartwig et al., 1992; He et al., 1997). As a consequence, in spite of the striking correlations between the effects of GMC and those of pharmacological agents that act on $PI(4,5)P_2$, some of the effects described in this study may be due to such direct interactions. The observation that the colocalization between GMC proteins and actin filaments is very limited (Wiederkehr et al., 1997) seems to argue against this possibility. In addition, under cell-free conditions, where filament decoration by other proteins was readily detectable by electron microscopy, we could not detect any decoration of actin monomers or filaments by recombinant GAP43 or CAP23 (Caroni, P., unpublished results). Therefore, although we presently cannot exclude more direct roles in actin dynamics regulation, we favor the possibility that interactions between GMC proteins and actin filaments may synergize with modulation of $PI(4,5)P_2$ to facilitate the recruitment and assembly of actin-based structures.

How does GMC-modulated $PI(4,5)P_2$ affect the actin cytoskeleton and cell-surface activity? Based on the results of this study, the fact that GMC expression correlates with cell cortex dynamics, and the known effects of $PI(4,5)P_2$ on the actin cytoskeleton and the cell cortex, we suggest that GMC levels affect local $PI(4,5)P_2$ availability, that in turn directly controls the activity of key actin regulating proteins. This model is consistent with recent evidence that $PI(4,5)P_2$ promotes membrane–cortical cytoskeleton interactions (Raucher et al., 2000), and that

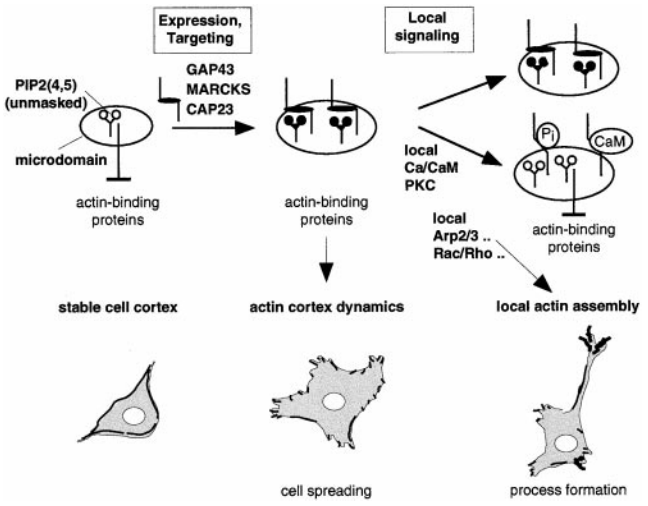

Figure 10. Proposed model of $PI(4,5)P_2$ modulation by GMC proteins at plasmalemmal microdomains, and its effects on actin cytoskeleton dynamics. Filled circles in the $PI(4,5)P_2$ symbols indicate masking by GMC; the bold segment in the GMC symbol indicates the basic domain; the bold lines at the cell periphery represent actin structures.

plasmalemmal actin polymerization promotes cell spreading (Vasioukhin et al., 2000). According to in vitro system studies, sequestration of $PI(4,5)P_2$ should consistently promote cell-surface actin dynamics, facilitating stimulus-induced actin recruitment, whereas its local liberation should promote growth and stabilization of peripheral actin structures (for reviews see Welch et al., 1997; Ma et al., 1998; Raucher et al., 2000). First, inhibition of gelsolin by $PI(4,5)P_2$ should reduce actin severing and dynamics (e.g., Hartwig et al., 1995). Second, global inhibition of cofilin by $PI(4,5)P_2$ should reduce monomer dissociation at the minus end of filaments, thus, reducing actin filament dynamics (Welch et al., 1997). Third, sequestration of profilin by $PI(4,5)P_2$ should globally inhibit filament growth, but promote local growth by uncapping filament plus ends (Hartwig et al., 1995). In addition, binding of WASP proteins to $PI(4,5)P_2$ promotes Arp2/3 function and actin recruitment, and binding of $PI(4,5)P_2$ to vinculin should promote focal contact formation.

The $PI(4,5)P_2$ modulatory mechanism suggested by our results is likely to be operating throughout the cell surface. Thus, although some local accumulation can be detected at sites of cell–substratum attachment and ruffling activity, the immunocytochemistry data suggest the presence of substantial amounts of evenly distributed $PI(4,5)P_2$ and GMC throughout the cell cortex. However, because it should be affected by the intrinsic, cell-specific properties of the cortical cytoskeleton, and by the local accumulation of structural, regulatory, and signaling components that initiate and regulate actin structure formation, its outcome is likely to exhibit highly cell specific and local features. Taking all these factors into account, actin regulation by GMC and $PI(4,5)P_2$ may involve the following mechanisms (see also Fig. 10). First, under local resting conditions, with low contents of components such as Arp2/3, CapZ, and activated Rho-type GTPases that promote the formation of dynamic structures, and with low levels of GMC proteins, accessible $PI(4,5)P_2$ would favor cortical actin cytoskeleton stability, suppressing local dynamics and inhibiting membrane fusion. Second, under the same conditions, but with higher levels of GMC proteins, $PI(4,5)P_2$ masking would lower the threshold for cell-surface dynamics, promoting processes such as cell spreading and membrane fusion. Third, in the presence of signals and components that promote the formation of actin structures, for example, at a forming axonal growth cone or phagosome, stimulus-induced release of $PI(4,5)P_2$ from masking by GMC would support local actin filament assembly, coupling this process to regulation by calcium/CaM and PKC signals. Overall, according to this model, the expression of proteins such as GAP43, MARCKS, or CAP23 would promote and regulate cell-surface dynamics, phagocytosis, cell attachment, and regulated morphogenic processes such as neurite outgrowth (Fig. 10). These predictions are in good agreement with a wealth of data from cultured cells and genetically modified mice.

The effects of GMC constructs on neurite outgrowth in PC12 cells, peripheral nerve regeneration, and stimulus-induced nerve sprouting at the neuromuscular junction of soleus muscle provide strong experimental evidence for a critical role of GMC proteins in promoting process outgrowth. Together with those of the accompanying paper (Frey et al. 2000a), they establish GMC proteins as major intrinsic determinants of anatomical plasticity in neurons. In addition, the results highlight the role of cell cortex regulation in controlling anatomical plasticity. Thus, overexpressing GAP43(ΔED) in neurons not only impaired proper axonal regeneration and synaptic sprouting, but also paradoxically allowed paralysis-induced sprouting at neuromuscular synapses that do not sprout in wild-type mice. Such sprouts were abnormal in shape and exhibited several features reminiscent of cytochalasin D–treated or CAP23−/− neurons. It is well established that disrupting the actin cytoskeleton of pioneer neurons in situ abolishes growth cone guidance and induces extensive twisted growth of neurites (Bentley and Toroian-Raymond, 1986). In a similar manner, intrinsic determination of anatomical plasticity in neurons may involve differential expression of components that control the dynamics of the actin cytoskeleton at the cell cortex, and interference with this control would disrupt specificity in stimulus-induced anatomical plasticity.

We thank S. Arber, J. Hagmann, W. Krek, and U. Mueller (Friedrich Miescher Institute), and E. Stoeckli (University of Basel) for valuable comments on the manuscript.

Submitted: 27 October 1999
Revised: 23 May 2000
Accepted: 24 May 2000

References

Aderem, A. 1995. The MARCKS family of protein kinase-C substrates. *Biochem. Soc. Trans.* 23:587–591.

Aigner, A., and P. Caroni. 1995. Absence of persistent spreading, branching, and adhesion in GAP-43–depleted growth cones. *J. Cell Biol.* 128:647–660.

Aigner, L., S. Arber, J.P. Kapfhammer, T. Laux, C. Schneider, F. Botteri, H.-R. Brenner, and P. Caroni. 1995. Overexpression of the neural growth-associated protein GAP-43 induces nerve sprouting in the adult nervous system of transgenic mice. *Cell.* 83:269–278.

Arber, S., T.A. Barbayannis, H Hanser, C. Schneider, C.A. Stanyon, O. Bernard, and P. Caroni. 1998. Regulation of actin dynamics through phosphorylation of cofilin by LIM-kinase. *Nature.* 393:805–809.

Baetge, E.E., and J.P. Hammang. 1991. Neurite outgrowth in PC12 cells deficient in GAP-43. *Neuron.* 6:21–30.

Benowitz, L.I., and A. Routtenberg. 1997. GAP-43: an intrinsic determinant of neuronal development and plasticity. *Trends Neurosci.* 20:84–91.

Bentley, D., and A. Toroian-Raymond. 1986. Disoriented pathfinding by pioneer neurone growth cones deprived of filopodia by cytochalasin treatment. *Nature.* 323:712–715.

Bird, I.M. 1998. Phospholipid signaling protocols. *Methods Mol. Biol.* 105:1–19.

Caroni, P. 1997. Overexpression of growth-associated proteins in the neurons of adult transgenic mice. *J. Neurosci. Methods.* 71:3–9.

Caroni, P., L. Aigner, and C. Schneider. 1997. Intrinsic neuronal determinants locally regulate extrasynaptic and synaptic growth at the adult neuromuscular junction. *J. Cell Biol.* 136:679–692.

Denisow, G., S. Wanaski, P. Luan, M. Glaser, and S. McLaughlin. 1998. Binding of basic peptides to membranes produces lateral domains enriched in the acidic lipids phosphatidylserine and phosphatidylinositol 4,5-bisphosphate: an electrostatic model and experimental results. *Biophys. J.* 74:731–744.

Frey, D., T. Laux, L. Xu, C. Schneider, and P. Caroni. 2000a. Shared and unique roles of Gap23 and Gap43 in actin regulation, neurite outgrowth, and anatomical plasticity. *J. Cell Biol.* 149:1443–1453.

Frey, D., C. Schneider, L. Xu, J. Borg, W. Spooren, and P. Caroni. 2000b. Early and selective loss of neuromuscular synapse subtypes with low sprouting competence in motoneuron diseases. *J. Neurosci.* 20:2534–2542.

Fukami, K., K. Matsuoka, O. Nakamshi, A. Yamakawa, S. Kawai, and T. Takenawa. 1988. Antibody to phosphatidylinositol 4,5,-bisphosphate inhibits oncogene-induced mitogenesis. *Proc. Natl. Acad. Sci. USA.* 85:9057–9061.

Han, J.K., K. Fukami, and R. Nuccitelli. 1992. Reducing inositol lipid hydrolysis, Ins(1,4,5)P3 receptor availability, or Ca^{2+} gradients lengthens the duration of the cell cycle in *Xenopus laevis* blastomeres. *J. Cell Biol.* 116:147–156.

Harder, T., and K. Simons. 1997. Caveolae, DIGs, and the dynamics of sphingolipid–cholesterol microdomains. *Curr. Opin. Cell Biol.* 9:534–542.

Harder, T., P. Scheiffele, P. Verkade, and K. Simons. 1998. Lipid domain structure of the plasma membrane revealed by patching of membrane components. *J. Cell Biol.* 141:929–942.

Hartwig, J.H., M. Thelen, A. Rosen, P.A. Janmey, A.C. Nairn, and A. Aderem. 1992. MARCKS is an actin filament crosslinking protein regulated by protein kinase C and calcium-calmodulin. *Nature.* 356:618–622.

Hartwig, J.H., G.M. Bokoch, C.L. Carpenter, P.A. Janmey, L.A. Taylor, A. Toker, and T.P. Stossel. 1995. Thrombin receptor ligation and activated Rac uncap actin filament barbed ends through phosphoinositide synthesis in permeabilized human platelets. *Cell.* 82:643–653.

He, Q., E.W. Dent, and K.F. Meiri. 1997. Modulation of actin filament behavior by GAP-43 (neuromodulin) is dependent on the phosphorylation status of serine 41, the protein kinase C site. *J. Neurosci.* 17:3515–3524.

Jackson, T.R., I.J. Beader, L.P. Hammonds-Odie, C.R. Burgon, F. Cooke, P.T. Hawke, A.G. Wolf, K.A. Heldmann, and A.B. Theibert. 1996. Inactivation and maintenance of HGF-stimulated neurite outgrowth requires activation of a phosphoinositide 3-kinase. *J. Cell Sci.* 109:289–300.

Liu, Y., L. Casey, and L.J. Pike. 1998. Compartmentalization of phosphatidylinositol 4,5-bisphosphate in low-density membrane domains in the absence of caveolin. *Biochem. Biophys. Res. Commun.* 245:684–690.

Ma, L., L.C. Cantley, P.A. Janmey, and M.W. Kirschner. 1998. Corequirement of specific phosphoinositides and small GTP-binding protein Cdc42 in inducing actin assembly in *Xenopus* egg extracts. *J. Cell Biol.* 140:1125–1136.

Maekawa, S., C. Sato, K. Kitajima, N. Funatsu, H. Kumanogoh, and Y. Sokawa. 1999. Cholesterol-dependent localization of NAP-22 on a neuronal membrane microdomain (raft). *J. Biol. Chem.* 274:21369–21374.

McNamara, R.K., and R.H. Lenox. 1997. Comparative distribution of myristoylated alanine-rich C kinase substrate (MARCKS) and F1/GAP-43 gene expression in the adult brain. *J. Comp. Neurol.* 379:48–71.

Meier, R., M. Thelen, and B.A. Hemmings. 1998. Inactivation and dephosphorylation of protein kinase Balpha (PKBalpha) promoted by hyperosmotic stress. *EMBO (Eur. Mol. Biol. Organ.) J.* 17:7294–7303.

Myat, M.M., S. Anderson, L.A. Allen, and A. Aderem. 1997. MARCKS regulates membrane ruffling and cell spreading. *Curr. Biol.* 7:611–614.

Olive, S., C. Dubois, M. Schachner, and G. Rougon. 1995. The F3 neuronal glycosylphosphatidylinositol-linked molecule is localized to glycolipid-enriched membrane subdomains and interacts with L1 and fyn kinase in cerebellum. *J. Neurochem.* 65:2307–2317.

Paves, H., T. Neuman, M. Metsis, and M. Saarma. 1990. Nerve growth factor-induced rapid reorganization of microfilaments in PC12 cells: possible roles of different second messenger systems. *Exp. Cell Res.* 186:218–226.

Penninger, J.M., and G.R. Crabtree. 1999. The actin cytoskeleton and lymphocyte activation. *Cell.* 96:9–12.

Pike, L.J., and J.M. Miller. 1998. Cholesterol depletion delocalizes phosphatidylinositol bisphosphate and inhibits hormone-stimulated phosphatidylinositol turnover. *J. Biol. Chem.* 273:22298–22304.

Raucher, D., T. Stauffer, W. Chen, K. Shen, S. Guo, J.D. York, M.P. Sheetz, and T. Meyer. 2000. Phosphatidylinositol 4,5-bisphosphate functions as a second messenger that regulates cytoskeleton-plasma membrane adhesion. *Cell.* 100:221–228.

Schafer, D., M.W. Welch, L.M. Machesky, P.C. Bridgman, S.M. Meyer, and J.A. Cooper. 1998. Visualization and molecular analysis of actin assembly in living cells. *J. Cell Biol.* 143:1919–1930.

Seki, K., F.-S. Sheu, and K.-P. Huang. 1996. Binding of myristoylated alanine-rich protein kinase C substrate to phosphoinositides attenuates the phosphorylation by protein kinase C. *Arch. Biochem. Biophys.* 326:193–201.

Skene, J.H.P. 1989. Axonal growth-associated proteins. *Annu. Rev. Neurosci.* 12:127–156.

Sretavan, D.W., and K. Kruger. 1998. Randomized retinal ganglion cell axon routing at the optic chiasm of GAP-43 deficient mice: association with midline recrossing and lack of normal ipsilateral axon turning. *J. Neurosci.* 18: 10502–10513.

Strittmatter, S.M., C. Fankhauser, P.L. Huang, H. Mashimo, and M.C. Fishman. 1995. Neuronal pathfinding is abnormal in mice lacking the neuronal growth cone protein GAP-43. *Cell.* 80:445–452.

Stumpo, D.J., C.B. Bock, J.S. Tuttle, and P.J. Blackshear. 1995. MARCKS deficiency in mice leads to abnormal brain development and perinatal death. *Proc. Natl. Acad. Sci. USA.* 92:944–948.

Tapon, N., and A. Hall. 1997. Rho, Rac and cdc42 GTPases regulate the organisation of the actin cytoskeleton. *Curr. Opin. Cell Biol.* 9:86–92.

Thelen, M., A. Rosen, A.C. Nairn, and A. Aderem. 1991. Regulation by phosphorylation of reversible association of a myristoylated protein kinase C substrate with the plasma membrane. *Nature.* 351:320–322.

Vasioukhin, V., C. Bauer, M. Yin, and E. Fuchs. 2000. Directed actin polymerization is the driving force for epithelial cell-cell adhesion. *Cell.* 100:209–219.

Welch, M.D., A. Mallavarapu, J. Rosenblatt, and T.J. Mitchison. 1997. Actin dynamics in vivo. *Curr. Opin. Cell Biol.* 9:54–61.

Wiederkehr, A., J. Staple, and P. Caroni. 1997. The motility-associated proteins GAP-43, MARCKS, and CAP-23 share unique targeting and surface activity-inducing properties. *Exp. Cell Res.* 236:103–116.

Yankner, B.A., L.I. Benowitz, L. Villa-Komaroff, and R.L. Neve. 1990. Transfection of PC12 cells with the human GAP-43 gene: effects on neurite outgrowth and regeneration. *Mol. Brain Res.* 7:39–44.